ELSEVIER

Journal of Alloys and Compounds 300–301 (2000) 131–140

Journal of ALLOYS AND COMPOUNDS

www.elsevier.com/locate/jallcom

Saturation effect on multiphonon relaxation rates of rare earth ions in glasses at high excitation power

F. Pellé*, F. Auzel

Groupe d'Optique des Terres Rares, LPCM-UPR 211 (CNRS), 1 Place A. Briand, 92195 Meudon Cedex, France

Abstract

An increase of the radiative quantum efficiency with increasing the excitation power is observed for several multiplets of rare earth ions in glasses. The effect of the excited state density on multiphonon relaxation rates is investigated for different rare earth excited states in oxide or fluoride based glasses. The multiphonon relaxation rate follows as usual an exponential gap law with a coefficient depending on the excited state density. A model is proposed to take into account for the saturation of the multiphonon process with increasing the excitation power. This bottleneck effect is related to the specific propagation, in disordered structures, of highly energetic vibrations resulting from the multiphonon process. Application of our model to optical data allows us to derive a phonon diffusion length which is in good agreement with the phonon mean free path estimated from thermal conductivity, heat capacity and sound velocity. Furthermore, the results are compared with the medium range order deduced from the frequency of the boson peak recorded in Raman scattering.

Keywords: Amorphous materials; Order–disorder effect; Phonons; Luminescence; Inelastic light scattering

1. Introduction

Radiationless processes by multiphonon relaxation in Rare Earth (RE) doped materials (crystal or glasses) have been extensively studied in an experimental and theoretical way since a long time. Different approaches were developed to calculate theoretically the *n*-phonon transition probability (linear mechanism [1–3], nonlinear mechanism [4–6], non adiabatic hamiltonian [7–11], inductive resonant theory [12]). For rare earth ions in a triply ionised state, the electron–phonon coupling is very low ($S_0 << 1$) and the assumption of the coupling with one phonon mode, i.e., the effective phonon model can be used. In this frame, the empirical exponential gap law describes well, in a first approximation, the experimental results on multiphonon relaxation rate with the number of phonons required to bridge the gap to the next lower state if the order of the process is less than 2. However, the use of powerful excitation sources such as pulsed laser providing a large number of excited ions can lead to discrepancy with the results obtained with a conventional low power excitation source. This underlines that high excited state density allows to observe new aspects of multiphonon relaxation processes. In this paper, we report the increase of the radiative quantum efficiency for several RE excited multiplets with increasing the number of excited ions in oxide and fluoride based glasses. We have already reported such an effect in a Yb^{3+} doped borate glass [13], and partially in germanate and tellurite glasses. The model we proposed to explain this bottleneck effect, is linked to the lowest step in the energy dissipation in the host i.e. the propagation of high energetic vibrations [14,15]. In this paper we extend the measurements to RE doped fluoride glass. Since no such effect has been found in crystals. This result reinforces our first assumption: the observed bottleneck effect on radiationless relaxation rate is related to an accepting modes saturation due to the localisation of energetic vibrations in glasses due to the disorder. The critical distance below which excited ions share a common phonon bath is related to the phonon diffusion length l_c in the host. From our model we deduce l_c. The results are compared with the phonon mean free path in the host deduced from sound velocity measurements and estimation of thermal conductivity and heat capacity. One another characteristic of disordered structure is the Boson peak recorded in the low frequency range, between 1 and 80 cm^{-1}, in Raman spectra. The low-frequency Raman scattering of light is due to the vibrational modes that are

*Corresponding author. Fax: +33-1-4507-51071.
E-mail address: pelle@cnrs-bellevue.fr (F. Pellé)

0925-8388/00/$ – see front matter
PII: S0925-8388(99)00743-4

localised by the disorder. From the position of the boson peak it is possible to derive a correlation length l corresponding to a medium range order in the glass [16]. The phonon diffusion lengths optically determined are well in the range of the correlation lengths deduced from Raman experiments.

2. Experimental

The phonon cut-off frequency of a glass is roughly that of the stretching vibration of their former group. So, we focus our interest on phosphate [$50(P_2O_5)$–$16.66(MgO)$–$33.34(Li_2O)$], germanate [$66(GeO_2)$–$17(BaO)$–$17(K_2O)$], tellurite [$80(TeO_2)$–$20(Li_2O)$] and ZBLAN [$57.35(Zr_4)$–$29.63(BaF_2)$ – $3.54(LaF_3)$ – $1.78(NaF)$ – $5.16(InF_3)$ – $2.54(AlF_3)$] glasses in order to get a phonon cut-off frequency varying from 1100 cm^{-1} to 560 cm^{-1}. Rare earth ions Er^{3+}, Tm^{3+}, Nd^{3+} and Ho^{3+} (in case of ZBLAN) were introduced in a low concentration (0.2 at.%) to avoid interactions and energy transfers. Moreover, in phosphate and ZBLAN glasses, the doping level was 2 at.% due to the weak quantum efficiency of the luminescence in the former case and weak non radiative probability due to the small phonon cut-off frequency in the latter case. RE multiplets were resonantly excited. The excitation was provided either by the second harmonic of a Nd:YAG laser or an OPO (pulse duration≈2.5 ns @ 600 nm) pumped by the third harmonic of a Nd:YAG, in the visible range. A pulsed Ti–Sapphire pumped by the frequency doubled Nd:YAG laser provided excitation of the relevant electronic states in the near infrared range. For high excitation powers, optical attenuators were used in front of the detectors to ensure a linear response of the system. The complete experimental set-up and procedure are described in [15]. From the beam diameter measured at the input face of the sample, the RE concentration (C) of each glass sample, the absorption cross section (σ) at λ_{exc} and the excitation power, the number of photons per pulse and area unit Q, derived from the mean power, the repetition rate of the laser pulses, the energy and the measured spot diameter of excitation, the excited state density is obtained through the following simple relation:

$$N_{exc} = \sigma C Q \quad (1)$$

The multiphonon relaxation rate W_{nr} is obtained, as usual, from experimental lifetime τ_{exp} and spontaneous emission decay τ_{rad} calculated from optical absorption and application of the Judd-Ofelt theory [17,18].

Raman spectra were excited with the argon ion laser emission at 457.9 nm. The scattered light was collected, at right angle, by lenses and dispersed by a triple monochromator (T800 Coderg).

3. Results

The lifetimes of the $Er^{3+}(^4S_{3/2})$, $Er^{3+}(^4I_{11/2})$, $Tm^{3+}(^3H_4)$ and $Nd^{3+}(^4F_{3/2})$ multiplets have been measured as a function of the excited state density, in all glass systems. Since the results obtained in oxide glasses have already been reported [15,19], we only briefly recall the main trends in order make a comparison with those obtained in ZBLAN.

The $^4S_{3/2}$ (Er^{3+}) state behaves in oxide based glasses in opposite way than in fluoride glasses. A shortening of the decay time, with increasing the excitation power, is observed in former cases otherwise lengthening is observed in ZBLAN. For example, in tellurite the experimental value measured at low excitation power is reduced by about 20% at high excitation power, while, in ZBLAN: Er (0.2%), τ_{exp} decreases by 9% of its initial value (Fig. 1).

Except the $^4S_{3/2}$ (Er^{3+}) state, we observe the same behaviour for all investigated levels. The $^4I_{11/2}$ (Er^{3+}), $^3H_4$ (Tm^{3+}) and $^4F_{3/2}$ (Nd^{3+}) decay times lengthen smoothly and monotonically with increasing the excitation power. As an example, the nonradiative quantum efficiency $\eta^{NR} = (\tau_{rad} - \tau_{exp})/\tau_{rad}$ of $^3H_4$ (Tm^{3+}) multiplet in tellurite, measured at low excitation power (0.41) is reduced to 0.03 at high excitation power. In germanate and tellurite glasses, the concentration of RE ions is low and contribution of energy transfer to the decay are negligible. The $^3H_4$ (Tm^{3+}) and $^4F_{3/2}$ (Nd^{3+}) states exhibit the largest energy gaps from the next lower levels and the probability of multiphonon transition is weak, in these cases, the experimental decay time approaches the radiative value calculated from absorption.

The behaviour of the decay times measured in the phosphate glass is the same over the excitation power range. Above a critical value, the decay time remains constant. This suggests that the non radiative relaxation by multiphonon process has been partially suppressed. However the time constant, at high excitation power, is still lower than the radiative one. In this case, the experiments are performed on a more concentrated sample, interactions between RE ions occur and their contribution to the nonradiative part of the decay cannot be reduced.

Nevertheless, in all cases, the observed variations are beyond the experimental accuracy of the measurements which is about 3%. Variations in experimental decays can arise either by amplified spontaneous emission (ASE), saturation or radiative trapping. No narrowing of the emission spectra is observed when increasing the excitation power [19]. Furthermore, the concentration of the RE in the glasses is weak and measurements on thin layers of powdered samples gives the same results. From these observations, AES and photon trapping can be ruled out.

In ZBLAN, out of the considered four excited states, only one of them yield useful results for the multiphonon emission rate determination versus the excitation power.

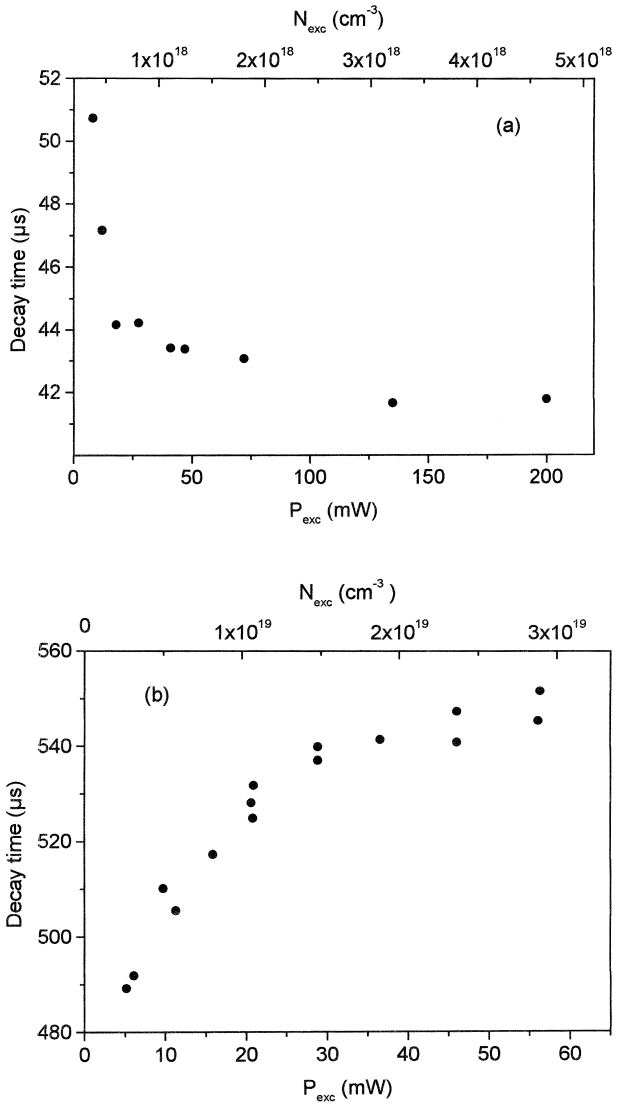

Fig. 1. $^4S_{3/2}$ (Er^{3+}) fluorescence decay time as a function of excitation power and excited state density in (a) tellurite glass, (b) ZBLAN.

With the exception of $^4S_{3/2}$, the energy gap from $^4I_{11/2}$, $^3H_4$ and $^4F_{3/2}$ levels to the next lower states are >3000 cm^{-1} and due to the low cut-off frequency of the host, the decays are predominantly radiative (especially for $^3H_4$ and $^4F_{3/2}$). In these cases, multiphonon emissions are negligible and their experimental time constant are equal to the determined radiative value within experimental error. To complete the set of the data in ZBLAN, $^4G_{7/2}(Nd^{3+})$, $^4I_{9/2}(Er^{3+})$ and $^5F_4(Ho^{3+})$ states which exhibit small gaps (1500, 2000 and 2600 cm^{-1} respectively) have been also considered. As shown on Fig. 2, the $^4G_{7/2}(Nd^{3+})$ decay increases with the excitation power. The experimental decay varies from 17 to 31 ns. The mean value is in good agreement with those recently reported in the same host [20]. The same effect is observed for the $^5F_4(Ho^{3+})$ multiplet (Fig. 3). The lifetime can be easily compared to the value determined in ZBLA [21]. The behaviour of the $^4I_{9/2}(Er^{3+})$ decay is more complex. In the range of moderate values of the excited state density, the decay decreases and then above $N_{exc}=1.5\times10^{19}$ cm^{-3} increases as it is observed for other levels. In this particular case, up-conversion is efficient and prevails over the saturation effect, thus reduces the decay time. At high excitation power, phonon bottleneck effect offsets up-conversion processes.

The multiphonon relaxation rates W_{nr} of $^4G_{7/2}(Nd^{3+})$, $^4I_{9/2}(Er^{3+})$, $^4S_{3/2}(Er^{3+})$ and $^5F_4(Ho^{3+})$ as a function of the excitation state density are represented in Fig. 4 respectively. As in germanate and tellurite glasses, a saturation of the non radiative decay rate due to multiphonon process is observed.

The complete study of the W_{nr} dependence with the energy gap, for a fixed value of the excited state density, is not possible in ZBLAN. First, to obtain a common range of excited state density for all the considered levels, the concentration of the RE, sometimes, has to be risen for the study of levels with a weak absorption cross-section. This has been possible in oxide based glasses where the high phonon cut-off frequency is such that multiphonon relaxation remains dominant in front of the up-conversion processes. Fluoride hosts are well-known to favour up-conversion effect which constitutes the main non radiative de-excitation path. In this case the concentration of the RE ions should remain rather low to avoid energy transfer.

In oxide based glasses, two main conclusions have been extracted from the W_{nr} dependence as a function of the multiphonon order process. First, for a given excited state density, the exponential gap law is followed. Increasing N_{exc} yields, on a semi-logarithmic scale, a set of lines with ascending slope. All of these lines intersect at the same point ($N\approx3$). In this point, the multiphonon relaxation rate does not depend on the excited state density. An analogous 'rotation' point has already been observed when comparing W_{nr} against the multiphonon order (N) for different hosts (crystals and glasses) [22]. Such behaviour had been predicted and attributed to the promoting modes which reduce the gap, the remaining energy being filled only by the accepting modes [11]. Our experimental results are consistent with this view and allow us to conclude that the initial step i.e. the enhancement of the non-radiative transition by the promoting modes is insensitive to the excited state density whereas the accepting modes start being saturated by the excited state density. This means that only multiphonon transitions requiring more than ≈3 phonons to bridge the electronic gap to the next lower level will saturate with the excitation power. The results, in turn, explain why the multiphonon relaxation rate of $^4S_{3/2}$ (Er^{3+}) in ZBLAN behaves in opposite direction than those obtained in other glasses since in this case, due to the small phonon cut off frequency, the $^4S_{3/2}$–$^4F_{9/2}$ energy gap has to be filled by about 4 or 5 phonons.

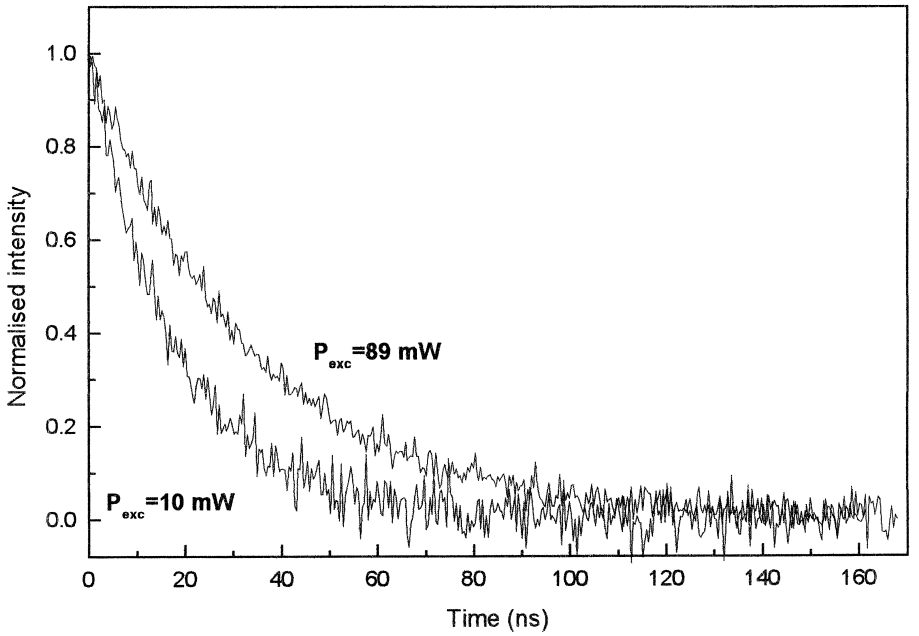

Fig. 2. $^4G_{7/2}$ (Nd^{3+}) fluorescence transient recorded at low and high excitation power in ZBLAN.

4. Multiphonon relaxation rate and excitation state density: a model

In the non adiabatic approach, multiphonon transitions, forbidden at first order in the adiabatic approximation, arise from the non adiabatic part of the hamiltonian (H_{NA}) applied to the Born Oppenheimer states. The total non-radiative probability W_{nr} for a N-phonon process between two quantum states, as given by the Fermi Golden rule, can be written as [10,11]:

$$W_{nr} = \frac{2\pi}{\hbar}|\langle i|H_{int}|j\rangle|^2 R_N \delta(E_j - E_i) \quad (2)$$

where $R_N\delta(E_j - E_i)$, given by the accepting modes term, represents the final density of states and R_N is the function first derived by Huang and Rhys [7]:

$$R_N = \exp[-(2\bar{n}+1)S_0]\left(\frac{\bar{n}+1}{\bar{n}}\right)^{N/2} I_N\left(2S_0\sqrt{\bar{n}(\bar{n}+1)}\right) \quad (3)$$

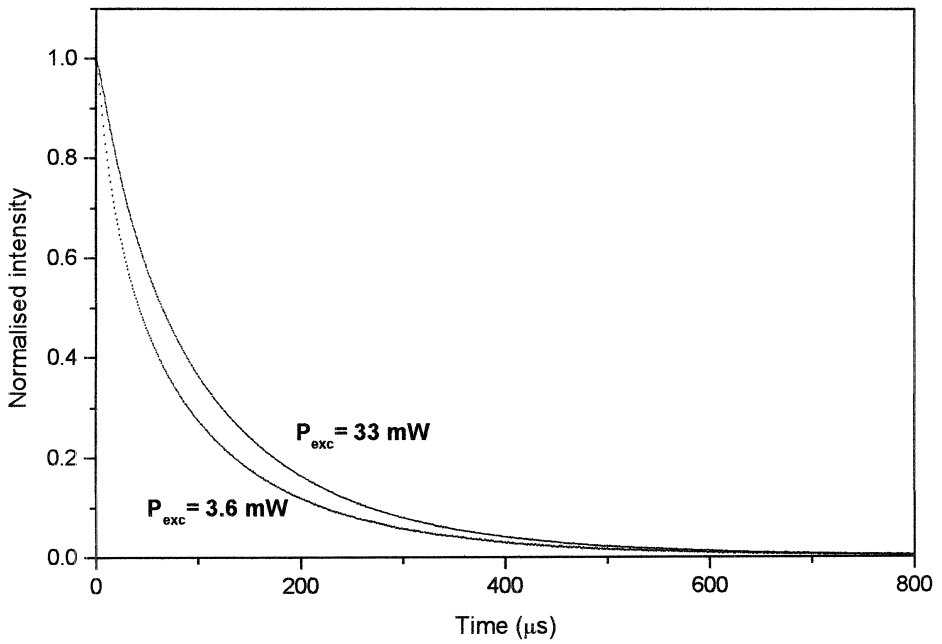

Fig. 3. $^5F_4$ (Ho^{3+}) fluorescence transient recorded at low and high excitation power in ZBLAN.

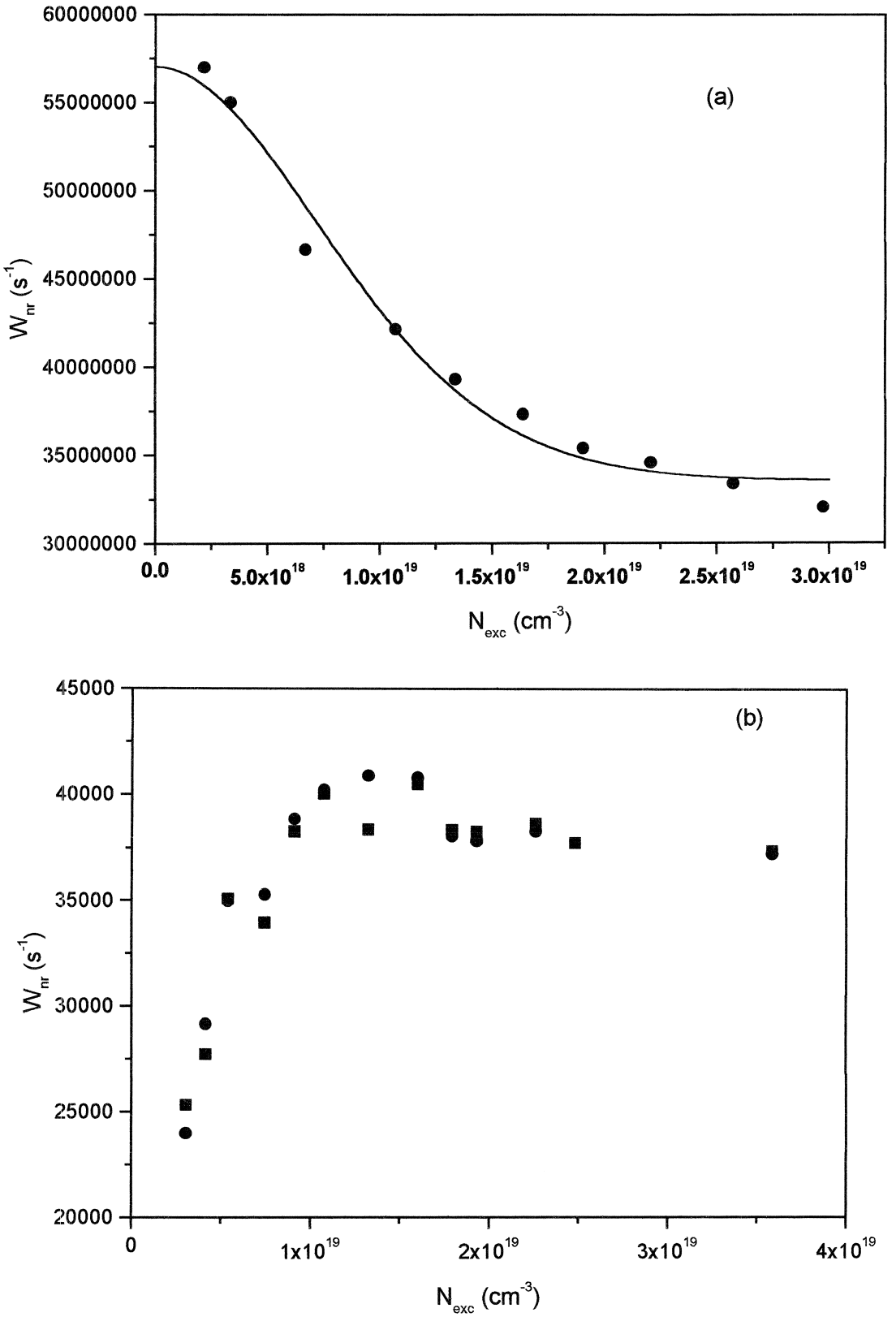

Fig. 4. Multiphonon relaxation rates of RE ions excited states in ZBLAN versus excited state population density (a) $^4G_{7/2}(Nd^{3+})$; (b) $^4I_{9/2}(Er^{3+})$; (c) $^4S_{3/2}(Er^{3+})$ and (d) $^5F_4(Ho^{3+})$. Theoretical fit of experimental data, plotted as solid lines, were obtained using Eq. (8).

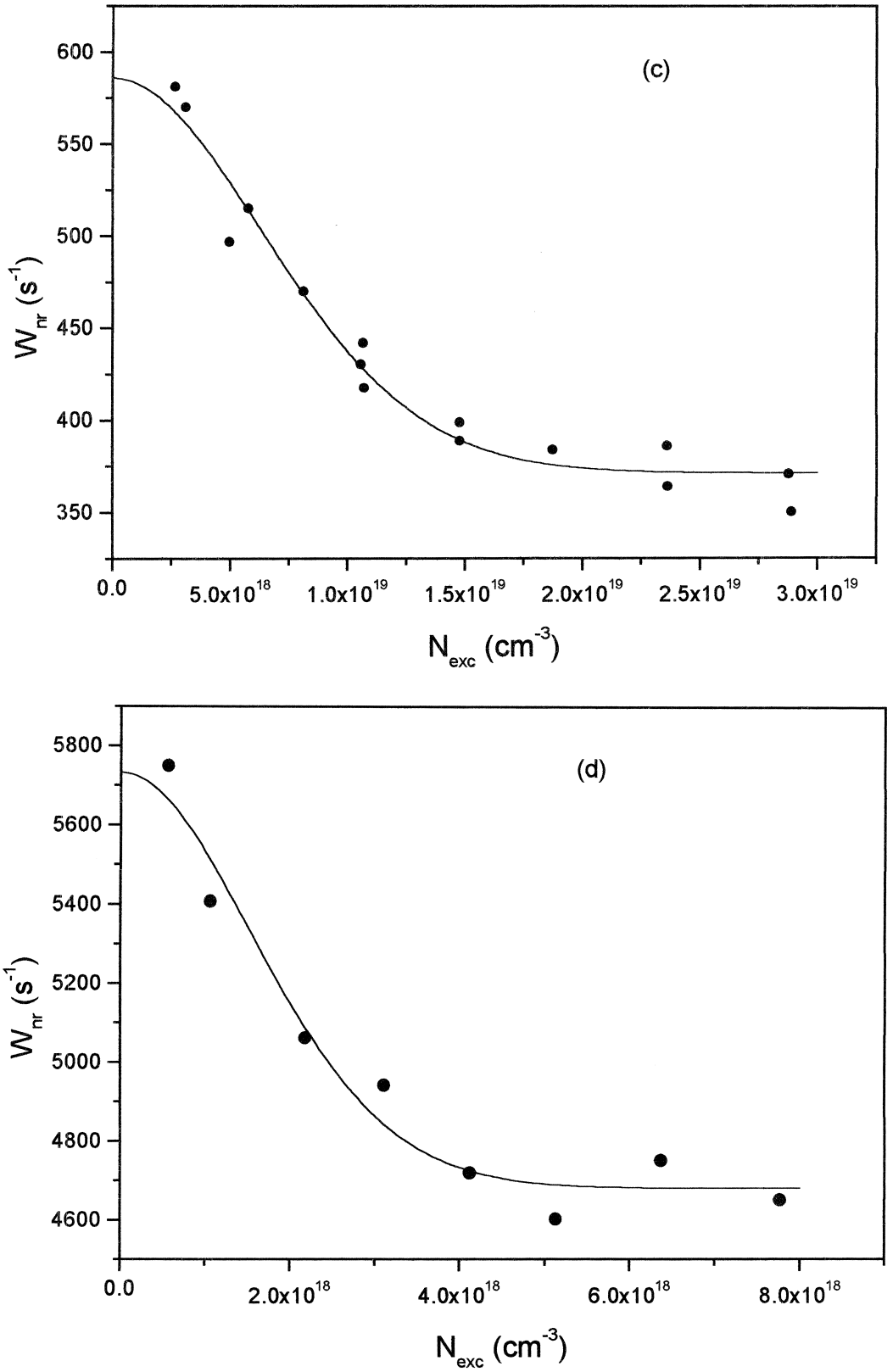

Fig. 4. (*continued*)

I_N is the modified Bessel function of order N and of complex argument, $\bar{n}$ the phonon occupation number. It has been shown [10,11] that in RE ions weak coupling case ($N >> S_0$), R_N can be simplified and including the promoting term W_{nr} is expressed as:

$$W_{nr} = \frac{2\pi}{\hbar}|\langle i(|H_{int}|j\rangle|^2 \exp[-S_0(2\bar{n}+1)](\bar{n}+1)^N \times \frac{S_0}{N!^N}\left(\frac{N_p}{S_0}\right)^2 \quad (4)$$

where N_p stands for the promoting modes.

Using Stirling's approximation, the factorial term gives the well-known exponential gap law:

$$W_{nr} = W_0 \exp[-\alpha \Delta E'] \quad (5)$$

where $\Delta E'$ is the energy gap to the next lower level reduced by the energy provided by the promoting modes ($2.6\ h\omega$) triggering the transition $\Delta E' = \Delta E - 2.6\ h\omega$ [16].

The promoting modes provide a translation on the energy scale as observed experimentally [22]. The accepting term has a statistical content and represents the probability of simultaneously filling, from the electronic energy, the N possible accepting modes of the host.

From our experimental results, the excited state population density should be taken into account in the multiphonon relaxation rate in order to explain the observed saturation of the radiationless transition probability. Increasing the excited state density, W_{nr} decreases exponentially with the energy gap, the slope of the semi-log plot varying with N_{exc}. The 'rotation' point has been related to the promoting term which remains unchanged by the excitation density [14,15]. To explain the behaviour of W_{nr} we propose the following process.

Since the excited state concentration increases with the excitation density, the averaged distance between two excited ions will obviously decrease. The distance at which two excited ions will share a common accepting phonon bath will depend on the phonon diffusion length l_c in the host. The volume for phonon diffusion common at least to two nearby excited ions will be defined as:

$$v_l = \frac{4\pi}{3} l_c^3 \quad (6)$$

On the assumption that RE ions are randomly distributed, with increasing the excitation density, an average of $\bar{x}$ will lie in the phonon diffusion volume around one excited ion. Then, $\bar{x}$ is proportional to the probability that a given excited ion can share with another excited ion a common sphere of radius l_c and is expressed in term of excited state density as:

$$\bar{x} = N_{exc} v_l [1 - \exp(-N_{exc} v_l)] \quad (7)$$

We suppose in this model that an average of $(1+\bar{x})$ ions instead of one will simultaneously fill the N common accepting modes set shared between the ions within a phonon diffusion volume. This effect can be simply described by substituting N by $(1+\bar{x})\ N$ in Eq. (4) only for the accepting term and not for the promoting one. The promoting modes are assumed, from our results, to stay localised and unchanged by the excitation density.

In this frame, the nonradiative decay probability as depending on the excitation state density is given by:

$$W_{nr} = W_0 \exp[-S_0(2\bar{n}+1)](\bar{n}+1)^{(1+\bar{x})N} \times \frac{S_0^{(1+\bar{x})N}}{[(1+\bar{x})N]!}\left(\frac{N_p}{S_0}\right)^2 \quad (8)$$

From Eq. (8), it is now possible to derive an expression for $\alpha = f(N_{exc})$ [15].

Applying Eq. (8) to the experimental relaxation rates obtained at different excited state densities, allows us to derive a phonon diffusion length. The least square fit of the data were performed with $\bar{x}$ as the only free parameter. We obtained 1.8 nm, 1.6 nm and 2.6 nm for $^4G_{7/2}(Nd^{3+})$, $^4S_{3/2}(Er^{3+})$ and $^5F_4(Ho^{3+})$ respectively. Theoretical curves are represented as continuous lines in Fig. 4. As we mentioned in Section 3, we have not obtained yet enough results to plot $W_{nr}^{N_{exc}} = f(N)$ in a wide range of N_{exc} values to derive a variation of α with N_{exc}. Complementary measurements on other multiplets, which gap corresponds to a multiphonon process order comprise between 2 and 5 and quite similar absorption cross-section, are in progress.

5. Discussion

Same kind of experiment has been performed for different states of Er^{3+} in a crystal ($SrLaGa_3O_7$). The fluorescence transient remain unchanged whatever the excitation power. This seems to confirm that the saturation of multiphonon process is closely related to the disordered structure of glasses. The main distinction between crystal and glass lies in the range of order which plays a dominant role for the scattering of phonons. In an ideal crystal, lattice dynamics shows that due to the periodicity of the host, the normal modes vibrations are wavelike with infinite extent. In a real crystalline sample due to various defects which act as damping factors for phonon propagation, the mode correlation functions are of finite extent but still extend over distances large compared with phonon mean free path in glasses. Due to the disorder in glasses, energetic phonons stay localised in a small volume. Multiphonon decay will result in an excess of high-energy phonons localised on the RE site and a local temperature well above that of the bath. To restore the thermal equilibrium of the lattice, these high frequency phonon modes will break into low frequency phonon modes due to anharmonic interactions within the lattice. The phonon mean free path will limit the rate of the energy dissipation. The observed bottleneck effect on radiationless transitions

is then related to the slowest step in the energy dissipation in glassy host.

In a thermodynamical approach, the phonon mean free path can be related to the thermal conductivity κ, the heat capacity C_v and the sound velocity v_s in the medium [23]. The amount of reliable practical data on the thermal conductivity of glasses being small, a rough estimation can be obtained by additive formulae based on derived oxide factors when available or an empirical relation based on density ρ [24]. The latter formulae

$$\kappa\ (\text{cal cm}^{-1}\,\text{s}^{-1}\,\text{deg}^{-1}) = \frac{0.005}{\rho} + 0.0004 \qquad (9)$$

has been used for our glasses. Eq. (9) enables thermal conductivities within the set of glasses for which κ is available to be calculated to 15%.

In the same way, the heat capacity is calculated with a good accuracy (10%) using additive formulae [25]provided all the constituent factors are known, i.e. for oxides. All the calculated values for the thermal conductivity and the heat capacity of our samples are summarised in Table 1 with the independently measured sound velocity. In case of ZBLAN, thermal conductivity and heat capacity were taken from literature [26,27]. The phonon mean free path is compared to the phonon diffusion lengths we obtained using our model for the different multiplets and from the a coefficient when available.

These results show that the crude one effective mode model for radiationless relaxation rates describes rather well the whole process even the energy dissipation from the effective mode towards lower energy modes. The observed bottleneck effect on nonradiative transitions is related to the slowest step in the energy dissipation in the host. It may take place between the high energy modes ruling the multiphonon process and the lower energy ones providing the final heating process.

Low frequency light scattering in glasses is strongly correlated to the specific propagation of vibrations in disordered structures. Amount of theoretical and experimental works are devoted, since the last two decades, to this property. In the following, Raman scattering experiments were performed on investigated glasses to get another link with the phonon diffusion length derived from spectroscopy and their medium range order.

6. Raman scattering

In Raman spectra, light scattering at low frequency (below 80 cm^{-1}) observed in glassy systems are due to the vibrational modes which are localised due to the disorder. The peak recorded in this range, often called boson peak, results from an excess of the vibrational density of states with respect to the Debye density of states. Several models have been proposed to interpret this phenomenon [28,29]. To interpret this excess, Duval [16] proposed a model based on a inhomogeneous medium made up of cohesive domains regions separated by weakly bonded regions. In this model, the vibrational frequency of a given domain is inversely proportional to its size 2a [16,28] following:

$$\omega_0 = \frac{s\nu_s}{(2a)c} \qquad (9)$$

with s a factor depending on the domain shape (0.5 for linear domains and 0.8 for spherical domains), v_s is the sound velocity in the host and c the speed of light in vacuum.

The boson peak were recorded on Raman spectra (Fig. 5) at 58, 41 and 48 cm^{-1} for the germanate, tellurite and ZBLAN glass respectively. It seems not realistic to have linear domains, so we will consider two values for the shape parameter $s = 0.65$ (mean value between linear and

Table 1
Phonon mean free path estimated from calculated thermal conductivity and specific heat, measured sound velocity and phonon diffusion length optically deduced

	κ $\left(\frac{\text{cal}}{\text{cm deg s}}\right)$	c_v $\left(\frac{\text{cal}}{\text{cm}^3\ \text{deg}}\right)$	v_s $\left(\frac{\text{cm}}{\text{s}}\right)$	l_c (nm)	l_{opt} (nm)	
Germanate	1.64×10^{-3}	0.445	3.81×10^{5}	2.9	α	2.9
					$^4I_{11/2}(Er^{3+})$	2.8
					$^3H_4(Tm^{3+})$	2.4
					$^4F_{3/2}(Nd^{3+})$	2.4
Tellurite	1.38×10^{-3}	0.852	2.40×10^{5}	2.0	α	2.2
					$^4I_{11/2}(Er^{3+})$	2.2
					$^3H_4(Tm^{3+})$	1.5
					$^4F_{3/2}(Nd^{3+})$	1.7
ZBLAN	1.673×10^{-3}	0.152	2.80×10^{5}	1.2	α	–
					$^4G_{7/2}(Nd^{3+})$	1.8
					$^4S_{43/2}(Er^{3+})$	1.6
					$^5F_4(Ho^{3+})$	2.6

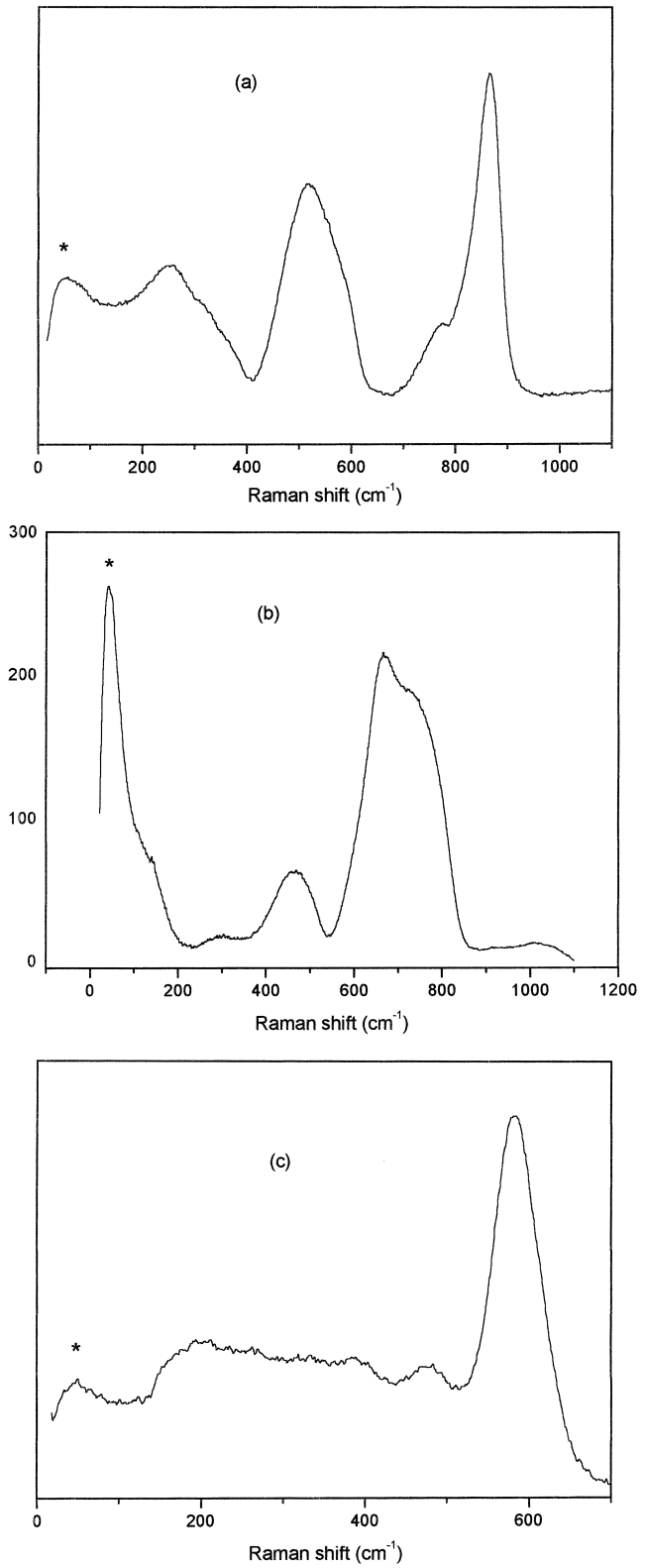

Fig. 5. Raman spectra of (a) germanate glass; (b) tellurite glass; (c) ZBLAN.

spherical shape) and $s=0.8$ for spherical domains. The size of the cohesive domains calculated using Eq. (9) and sound velocities experimentally determined for both values of s are summarised in Table 2. Except for the $^5F_4$ (Ho^{3+}) state in ZBLAN, these values are well in the range of the phonon diffusion lengths optically derived and phonon mean free path estimated from thermal conductivity, heat capacity and sound velocity. All the results seem to give a phonon diffusion length decreasing from the germanate to the ZBLAN. The discrepancy of the data in case of $^5F_4$(Ho^{3+}) with other multiplets in ZBLAN cannot be interpreted. Inhomogeneity or structural modification of the glass by introduction of Ho^{3+} can explain the results.

Table 2
Boson peak frequency and correlation length

	ω_0 (cm^{-1})	$2a$ (nm) $s=0.65$	$2a$ (nm) $s=0.8$
Germanate	58	1.4	1.7
Tellurite	41	1.3	1.6
ZBLAN	48	1.3	1.5

7. Conclusion

Saturation of multiphonon relaxation rate of RE multiplets is observed in oxide and fluoride based glasses. The bottleneck effect seems to be a general trend in disordered materials. A model is proposed to explain the W_{nr} dependence with excited state density for individual levels and the dependence of the α parameter of the exponential gap law with N_{exc}. Experimental difficulties inherent with the low phonon cut-off frequency of fluorides did not allow to extend the study on the α coefficient in ZBLAN. However, the phonon diffusion lengths deduced from optical data have been compared with the phonon mean free path deduced from thermal conductivity, heat capacity and sound velocity. The end result still point to the fact that the bottleneck effect is linked to the phonon mean free path which limits the energy dissipation in a glassy host. An estimation of the structural correlation length is proposed from the boson peak recorded in the low frequency range on Raman spectra.

Acknowledgements

This work is partially supported by INTAS grant No 96-0232. We would like to thank Denise Morin and Monique Genotelle for synthesis of the samples, density and refractive indexes measurements. Nicole Gardant for absorption and Raman experiments.

References

[1] H.W. Moos, J. Lumin. 1/2 (1970) 106.
[2] W.E. Hagston, J.E. Lowther, Physica 70 (1973) 40.

[3] L.A. Riseberg, M.J. Weber, Relaxation phenomena in rare-earth luminescence, in: E. Wolf (Ed.), Progress in Optics, Vol. XIV, North Holland, 1976, pp. 91–159.
[4] A. Kiel, Line Broadening in the Excited State of Paramagnetic Crystals, in: W. Low (Ed.), Paramagnetic Resonance, Academic, New York, 1963, pp. 525–534.
[5] K.K. Pukhov, V.P. Sakhun, Phys. Stat. Sol. B 95 (1979) 391.
[6] Y.V. Orlovskii, K.K. Pukhov, T.T. Basiev, T. Tsuboi, Opt. Mat. 4 (1995) 583.
[7] K. Huang, A. Rhys, Proc. R. Soc. London, A 204 (1950) 406.
[8] M. Lax, J. Chem. Phys. 20 (1952) 1752.
[9] R. Kubo, Y. Toyozawa, Progr. Theor. Phys. 13 (1955) 160.
[10] T. Miyakawa, D.L. Dexter, Phys. Rev. B 1 (1970) 2661.
[11] F. Auzel, Multiphonon interaction of excited luminescent centres in the weak coupling limit: non radiative decay and multiphonon side bands, in: B. Di Bartolo (Ed.), Luminescence of Inorganic Solids, Plenum, New York, 1978, pp. 67–113.
[12] V.L. Ermolaev, E.B. Sveshnikova, Opt. Spektrosk. 30 (1971) 379.
[13] F. Auzel, F. Pellé, J. Lumin. 69 (1996) 249.
[14] F. Auzel, F. Pellé, J. Phys. Rev. B 55 (1997) 11006.
[15] F. Pellé, N. Gardant, F. Auzel, J. Opt. Soc. Am. B 15 (1998) 667.
[16] E. Duval, A. Boukenter, B. Champagnon, Phys. Rev. Lett. 56 (1986) 2052.
[17] B.R. Judd, Phys. Rev. 127 (1962) 750.
[18] G.S. Ofelt, J. Chem. Phys. 37 (1962) 511.
[19] F. Pellé, N. Gardant, F. Auzel, J. Alloys Comp. 275/277 (1998) 430.
[20] S.A. Payne, C. Bibeau, J. Lumin. 79 (1998) 143.
[21] R. Reisfeld, M. Eyal, E. Greenberg, C.K. Jorgensen, Chem. Phys. Lett. 118 (1985) 25.
[22] J.M.F. Van Dijk, M.F.H. Schuurmans, J. Chem. Phys. 78 (1983) 5317.
[23] C. Kittel (Ed.), Introduction to Solid State Physics, J. Wiley, New York, 1971.
[24] E.H. Ratcliffe, Glass Technol. 4 (1963) 113.
[25] H. Scholze (Ed.), GLAS, Natur, Struktur und Eigenschaften, Springer Verlag, Berlin/Heidelberg, 1977.
[26] D.L. Davin, K.H. Chung, A.J. Bruce, C.T. Moynihan, J. Am. Ceram. Soc. 65 (1982) c182.
[27] A.J. Bruce, in: R. Almeida (Ed.), NATO ASI E: Applied Sciences, Vol. 123, 1985, p. 157.
[28] E. Duval, A. Boukenter, T. Achibat, J. Phys.: Condens. Matter 2 (1990) 10227.
[29] A.P. Sokolov, A. Kislink, M. Soltwistch, D. Quitmann, Phys. Rev. Lett. 69 (1992) 1540.